Cardiovascular Research (2014) **102**, 487–496
doi:10.1093/cvr/cvu055

Disease and region-related cardiac fibroblast potassium current variations and potential functional significance

Chia-Tung Wu[1,2], Xiao-Yan Qi[1], Hai Huang[1], Patrice Naud[1], Kristin Dawson[1,3], Yung-Hsin Yeh[2], Masahide Harada[1,4], Chi-Tai Kuo[2], and Stanley Nattel[1,3]*

[1]Research Center, Montreal Heart Institute, Université de Montréal, 5000 Belanger St. E., Montreal, QC, Canada H1T 1C8; [2]Chang-Gung Memorial Hospital and University, Taoyuan, Taiwan, Republic of China; [3]Department of Pharmacology and Therapeutics, McGill University, Montreal, QC, Canada; and [4]Department of Cardiology, Hamamatsu Medical Center, Hamamatsu, Japan

Received 24 May 2013; revised 25 February 2014; accepted 26 February 2014; online publish-ahead-of-print 4 March 2014

Time for primary review: 20 days

Aims Fibroblasts, which play an important role in cardiac function/dysfunction, including arrhythmogenesis, have voltage-dependent (Kv) currents of unknown importance. Here, we assessed the differential expression of Kv currents between atrial and ventricular fibroblasts from control dogs and dogs with an atrial arrhythmogenic substrate caused by congestive heart failure (CHF).

Methods and results Left atrial (LA) and ventricular (LV) fibroblasts were freshly isolated from control and CHF dogs (2-week ventricular tachypacing, 240 bpm). Kv currents were measured with whole-cell voltage-clamp, mRNA by quantitative polymerase chain reaction (qPCR) and fibroblast proliferation by ^{3}H-thymidine incorporation. Robust voltage-dependent tetraethylammonium (TEA)-sensitive K^+ currents (IC_{50} ~1 mM) were recorded. The morphologies and TEA responses of LA and LV fibroblast Kv currents were similar. LV fibroblast Kv-current densities were significantly greater than LA, and Kv-current densities were significantly less in CHF than control. The mRNA expression of Kv-channel subunits Kv1.5 and Kv4.3 was less in LA vs. LV fibroblasts and was down-regulated in CHF, consistent with K^+-current recordings. Ca^{2+}-dependent K^+-channel subunit (KCa1.1) mRNA and currents were less expressed in LV vs. LA fibroblasts. Inhibiting LA fibroblast K^+ current with 1 mmol/L of TEA or KCa1.1 current with paxilline increased proliferation.

Conclusions Fibroblast Kv-current expression is smaller in CHF vs. control, as well as LA vs. LV. KCa1.1 current is greater in LA vs. LV. Suppressing Kv current with TEA enhances fibroblast proliferation, suggesting that Kv current might act to check fibroblast proliferation and that reduced Kv current in CHF may contribute to fibrosis. Fibroblast Kv-current remodelling may play a role in the atrial fibrillation (AF) substrate; modulating fibroblast K^+ channels may present a novel strategy to prevent fibrosis and AF.

Keywords Fibroblast • Ionic channel • Congestive heart failure • Remodelling • Proliferation

1. Introduction

Cardiac fibroblasts constitute ~65–70% of cells in the heart.[1] Fibroblasts are crucial for maintaining the cardiac extracellular matrix skeleton. They also produce autocrine and paracrine factors that contribute to cell signalling and affect cardiomyocyte impulse conduction and ion-channel expression.[2] Under stimuli like stretch, ischaemia, or infection, cardiac fibroblasts can proliferate and differentiate into a highly secretory myofibroblast phenotype, which expresses organized α-smooth muscle actin.[3,4] Fibrosis increases myocardial stiffness, causing diastolic dysfunction. Fibrosis may also delay impulse conduction and facilitate arrhythmias like atrial fibrillation (AF) and ventricular tachycardia.[5,6]

Although fibroblasts and myofibroblasts are inexcitable, cardiomyocyte–fibroblast electrical coupling has been demonstrated both *in situ* and *in vitro*,[7,8] with both gap junctions and nanotubes potentially involved.[9] Fibroblasts possess mechanosensitive channels that can respond to myocyte contraction and change fibroblast membrane potential.[10,11]

* Corresponding author. Tel: +1 514 376 3330; fax: +1 514 376 1355, Email: stanley.nattel@icm-mhi.org

Multiple ion currents are present in cardiac fibroblasts, with distributions and properties quite distinct from cardiomyocytes.[4,12] There is evidence that fibroblast ion channels may be involved in governing proliferation and differentiation. Ventricular fibroblasts express a variety of Kv channel α-subunits and Kir current, and changing extracellular K^+ concentration can affect physiological functions such as survival and proliferation.[4,13] In many heart disease paradigms, the atria show a stronger fibrotic response than ventricles,[14,15] with at least some of this difference due to intrinsically different responses of atrial and ventricular fibroblasts to pathological stimuli like platelet-derived growth factor (PDGF), basic fibroblast growth factor, angiotensin II, endothelin 1, and transforming growth factor beta-1.[15] Pathological processes like congestive heart failure (CHF) can dramatically increase atrial fibrous tissue expression, creating a substrate for AF.[5,13,15]

To date, there has been no comparative analysis of ion-channel expression and properties between atrial and ventricular fibroblasts. In addition, the potential functional significance of fibroblast ion-channel changes in CHF has not been studied. We hypothesized that differential expression of voltage-gated (Kv) fibroblast K^+ channels might exist between atrium and ventricle and/or between normal and CHF hearts, and that such differences might affect functional fibroblast properties. We therefore performed whole-cell patch-clamp studies on freshly isolated fibroblasts from control and CHF canine hearts. Ventricular tachypacing was used to induce CHF, as in previous work.[5,14–16] To study the potential functional significance, we applied K^+-channel blockers on cultured fibroblasts and used ^{3}H-labelled thymidine assays to measure effects on fibroblast proliferation.

2. Methods

2.1 Animal model

Animal handling procedures followed the National Institutes of Health guidelines and were approved by the Animal Research Ethics Committee of the Montreal Heart Institute. Adult male mongrel dogs (weight 25–35 kg) were studied (control group $n = 32$, mean weight: 23.1 ± 0.5 kg; CHF group $n = 18$, 22.9 ± 0.7 kg; see Supplementary material online, *Figure S1A*). CHF dogs underwent subcutaneous pacemaker (St. Jude Medical) implantation under acepromazine (0.07 mg/kg IM)/diazepam (0.25 mg/kg IV)/ketamine (5.3 mg/kg IV)–premedication/isoflurane (1.5%) anaesthesia, with bipolar pacing leads inserted into the right-ventricular apex via a jugular vein. After 24-h recovery from surgery, dogs were ventricular-paced at 240 bpm for 2 weeks.[14] Before haemodynamic studies, all dogs were intubated and anaesthetized [acepromazine 0.07 mg/kg IM, diazepam 0.25 mg/kg IV, ketamine 5.3 mg/kg IV; following premedication with isoflurane (1.5%)]. The heart was exposed via a median sternotomy. The blood pressure was obtained from an arterial line in the right femoral artery. Left atrial and ventricular pressures were measured by a direct puncture with an 18-G needle. CHF dogs had significantly lower systolic blood pressure (112 ± 15 vs. 139 ± 12 mm Hg, $P < 0.001$) and higher left ventricular end-diastolic pressure (14.6 ± 1.9 vs. 5.9 ± 0.5 mm Hg, $P < 0.001$), compared with control dogs (see Supplementary material online, *Figure S1B*). After haemodynamic study, the heart was excised for cell isolation.

2.2 Fibroblast isolation

Dogs were anaesthetized with intravenous morphine (2 mg/kg) and α-chloralose (120 mg/kg). The left atrium (LA) and adjacent left ventricle (LV) were removed and placed in Tyrode solution containing (in mmol/L): NaCl 136, KCl 5.4, $MgCl_2$ 1, $CaCl_2$ 2, NaH_2PO_4 0.33, HEPES 5, and dextrose 10, pH 7.35 (adjusted with NaOH). The left circumflex coronary artery was perfused at ∼50 mL/min with Tyrode solution, followed by Ca^{2+}-free Tyrode for 10 min. The preparation was then perfused with Ca^{2+}-free Tyrode solution containing Type II collagenase (150 U/mL) plus 0.1% albumin for 1 h. Digested LA and LV tissue was harvested, carefully minced and agitated, centrifuged at 54.6 *g* for 3 min, and then passed through a 30 μm nylon filter to remove cardiomyocytes. Cell suspensions were examined microscopically to ensure <1% cardiomyocyte contamination. The remaining cell suspension was then centrifuged at 314.5 *g* for 10 min, and the fibroblast-rich sediment collected.

2.3 Cellular electrophysiology

Freshly isolated LA and LV fibroblasts were suspended in Kraft-Brühe (KB) solution containing (in mmol/L) KCl 20, KH_2PO_4 10, dextrose 10, mannitol 40, L-glutamic acid 70, β-OH-butyric acid 10, taurine 20, and EGTA 10 and 0.1% BSA (pH 7.3, KOH), and maintained at room temperature. Whole-cell patch clamp was performed at 34 ± 1°C, except when measuring K^+ reversal potential, which was performed at room temperature (20 ± 2°C) to resolve tail currents. Borosilicate glass microelectrodes with tip resistances between 5 and 10 MΩ were filled with nominally Ca^{2+}-free internal solution containing (in mmol/L) GTP 0.1, K^+-aspartate 110, KCl 20, $MgCl_2$ 1, ATP-Mg 5, HEPES 10, Na_2-phosphocreatine 5, and EGTA 0.05, pH 7.4 (adjusted with KOH). To record membrane potential, nystatin (600 μg/mL) was used to perform perforated patch recording. The bath solution was Tyrode solution with 2 mmol/L of $CaCl_2$. Currents were recorded with a holding potential of −40 mV and 300 ms voltage steps with 10 mV increments. Membrane voltages were corrected for the mean junction potential of 10.4 mV.

2.4 Real-time quantitative polymerase chain reaction

Paired LA and LV purified fibroblast pellets from each animal were flash-frozen in liquid N_2 for subsequent RNA isolation. The frozen pellet was later resuspended in lysis buffer, and the mRNAs were isolated using Nucleospin RNA II (Macherey Nagel), including DNase treatment to prevent genomic contamination. mRNA was reverse-transcribed with the High-capacity Reverse Transcription kit (Applied Biosystems). Quantitative polymerase chain reaction (qPCR) was performed with TaqMan probes and primers from Applied Biosystems for the housekeeping genes hypoxanthine-guanine phosphoribosyltransferase (HPRT; Cf02626258_m1), beta-2-microglobulin (Cf02659077_m1), and glucose-6-phosphate dehydrogenase (G6PD; Cf02646196_m1); as well as KCa1.1 (Cf0268385_m1). We designed primers for SyBr Green studies to assess the mRNA expression of Kv1.5 and Kv4.3 (see Supplementary material online, *Table S1*). The average of the expressions of HPRT, beta-2-microglobulin, and G6PD was used as the internal standard for qPCR. qPCR was performed with Taqman Gene Expression Master Mix and Power Sybr Green kits (Applied Biosystems). Reactions were run on a Stratagene MX3000. Relative gene expression values were calculated by the $2^{-\Delta C_t}$ method for the Taqman assays, and by $E^{-\Delta C_t}$ for the SyBr Green experiments.

2.5 Cell culture and ^{3}H-labelled thymidine incorporation assay

Freshly isolated fibroblasts from control dogs were collected and cultured in standard Medium 199 with 10% foetal bovine serum for 4–5 days, and then transferred to 24-well plates at 3×10^4 cells per well. The cells were incubated in serum-free Medium 199 for 24 h to synchronize cell cycle, followed by treatment with tetraethylammonium (TEA; 0.1 or 1 mmol/L), 4-AP (300 μmol/L), S9947 (1 μmol/L), or paxilline (0.1 or 1 μmol/L) for another 24 h. ^{3}H-labelled thymidine was applied (1 μCi per well) during the last 4 h of treatment. Before measurement, the cells were processed with trichloroacetic acid and NaOH. The mixture from each well was transferred to a 20 mL tube containing scintillation fluid and ^{3}H-disintegrations per minute (DPM) were counted 24 h later.

2.6 Statistical analysis

Data analysis was performed with Microsoft Excel 2003, Axon Clampfit 9, and Graphpad Prism 5. Results are presented as mean ± SEM. Unpaired Student's *t*-tests were used for two group comparisons. To compare current–voltage (*I–V*) relationships, K^+-channel subunit mRNA expression and ^{3}H-DPM proliferation indices between CHF and control, or different drug and control groups, two-way ANOVA, was performed. Bonferroni-corrected *t*-tests were used to assess individual-mean differences in fibroblast proliferation and subunit mRNA expression. A two-tailed *P*-value of ≤ 0.05 was considered statistically significant.

3. Results

3.1 Basic cellular parameters of freshly isolated atrial and ventricular fibroblasts

Freshly isolated canine LA and LV fibroblasts were spherical or slightly oval in shape (see Supplementary material online, *Figure S2A*). There were no gross morphological differences between LA and LV fibroblasts. The mean cell diameters were 9.5 ± 0.1 and 9.6 ± 0.2 μm for LA and LV fibroblasts, respectively (P = NS, see Supplementary material online, *Figure S2B*). Cell capacitances averaged 12.4 ± 0.7 pF for LA vs. 12.7 ± 0.7 pF for LV fibroblasts (P = NS, see Supplementary material online, *Figure S2C*). The resting membrane potential assessed by whole-cell perforated patch-clamp (corrected for a junction potential of 10.4 mV between pipette and bath solution) averaged −42.8 ± 1.3 mV for LA and −44.9 ± 1.7 mV for LV fibroblasts (P = NS, see Supplementary material online, *Figure S2D*). Compared with control fibroblasts, CHF fibroblasts showed significantly greater cell diameter (LA fibroblasts: 12.6 ± 0.4 μm, LV fibroblasts: 12.4 ± 0.3 μm; vs. 9.5 ± 0.1 and 9.6 ± 0.2 μm in control, respectively) and larger cell capacitance (LA fibroblasts: 18.9 ± 1.0 pF, LV fibroblasts: 18.4 ± 0.9 pF; vs. 12.4 ± 0.7 and 12.7 ± 0.7 pF). LA fibroblasts from CHF dogs had significantly more negative membrane potentials than those from control dogs (−50.0 ± 1.2 vs. −42.8 ± 1.3 mV, $P < 0.05$). Resting potential differences between control and CHF LV fibroblasts were not statistically significant (−44.9 ± 1.7 vs. −49.9 ± 2.1 mV, P = NS).

3.2 Kv currents in freshly isolated fibroblasts

Typical fibroblast currents are illustrated in *Figure 1A*, with rapidly activating and slowly inactivating kinetics. *Figure 1B* shows the response to 30 mmol/L of TEA (NaCl concentration was reduced to 106 mmol/L to maintain constant osmolarity). TEA blocked 83 ± 2% of the current at +60 mV (n = 15 cells), with the effect being reversible (*Figure 1C*). To confirm that the current is predominantly carried by K^+, we investigated the reversal potential based on tail current measurements at extracellular K^+ concentration ($[K^+]_o$) values of 5, 20, and 100 mmol/L (with NaCl concentration modified accordingly to maintain constant osmolarity). Following a 100 ms step from the holding potential (−40 mV), tail current was recorded during 1000 ms voltage steps, as illustrated in *Figure 1D*. The experiment was conducted at room temperature to slow inactivation and clearly resolve tail currents. The reversal potential was −58.2 mV in 5 mmol/L of $[K^+]_o$, −42.3 mV in 20 mmol/L of $[K^+]_o$, and −4.1 mV in 100 mmol/L of $[K^+]_o$ (*Figure 1E*). A log plot of the reversal potentials and the best-fit regression line (dotted) are shown in *Figure 1E*. The slope of the best-fit line was 41.9 vs. 58.1 mV predicted from the Nernst equation (solid line in *Figure 1E*) at $[K^+]_i$ = 130 mmol/L. The deviation from the Nernst equation suggests either imperfect Kv-current selectivity for K^+ or that TEA blocked other currents.

3.3 Kv-current differences between LA and LV fibroblasts

Figure 2A shows whole-cell end-pulse current density vs. voltage relations obtained in parallel from paired LA and LV fibroblasts from individual dogs. To compare mean LA cell current density with mean LV cell current density on a per-dog basis, we averaged all LA cell results for each control dog and all LV cell results from the same dog, and compared the resulting *I–V* curves. Statistically significant LA–LV differences were apparent: LV fibroblasts expressed significantly larger current densities than LA. TEA-sensitivity was tested in both LA and LV fibroblasts, to get a sense of whether there might be qualitative differences in their Kv currents. There were no significant LA–LV differences in TEA response at any concentration (*Figure 2B*). The estimated 50% inhibitory concentrations (IC_{s50}) for TEA were 0.7 mmol/L in LA and 1.1 mmol/L in LV fibroblasts. We also verified the current sensitive to 4-AP (at 300 μmol/L, *Figure 2C*) and the selective Kv 1.5 channel blocker S9947 (1 μmol/L, *Figure 2D*)[17] in fibroblasts. LV fibroblasts showed significantly larger 4-AP-sensitive current (e.g. 61% larger at +70 mV) and S9947-sensitive current (e.g. 49% larger at +70 mV) than LA fibroblasts.

3.4 Effects of CHF

Figure 3A (left panel) shows Kv currents from a CHF fibroblast before and after 30 mmol/L of TEA. The overall pre-drug morphology was similar to that of control fibroblast Kv currents, although the amplitude was smaller. TEA strongly inhibited the current (*Figure 3A*), similar to the response in control fibroblasts. There were no statistically significant differences in current density between LA and LV CHF fibroblasts (*Figure 3B*). *Figure 3C* shows a comparison of 30-mmol/L TEA-sensitive current densities between control and CHF fibroblasts. Fibroblasts from CHF dogs expressed significantly smaller Kv currents compared with those from control dogs, both for LA (e.g. 3.1 ± 0.5 CHF vs. 7.0 ± 0.8 pA/pF control at +60 mV, $P < 0.001$) and LV fibroblasts (e.g. 3.5 ± 0.7 CHF vs. 8.9 ± 1.1 pA/pF control at +60 mV, $P < 0.001$). Similar to control fibroblasts, 4-AP- (at 300 μmol/L, see Supplementary material online, *Figure S3A*) and S9947- (at 1 μmol/L, see Supplementary material online, Figure S*3B*) sensitive currents were significantly larger in CHF LV fibroblasts vs. CHF LA fibroblasts.

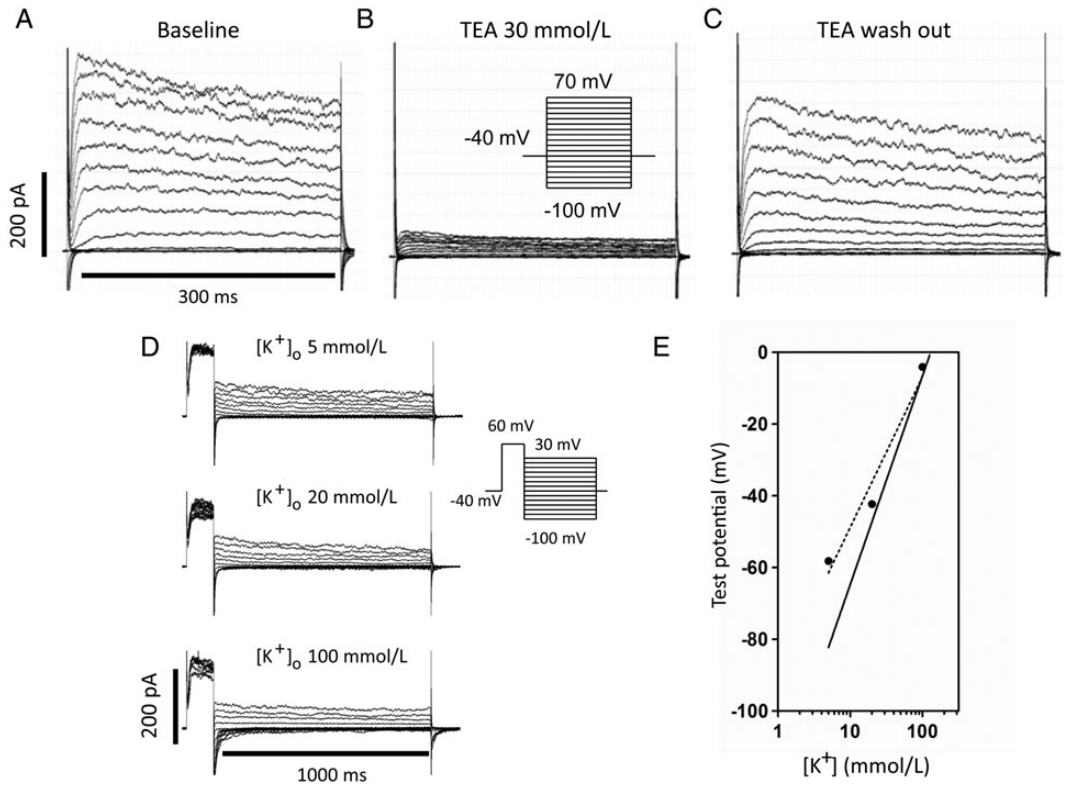

Figure 1 Representative currents recorded from control cardiac fibroblasts are shown at baseline (*A*), after treatment with TEA 30 mmol/L (*B*), and wash-out of TEA (*C*). (*D*) Representative tail current recordings at different extracellular K^+ concentration ($[K^+]_o$) values: 5, 20, and 100 mmol/L. (*E*) Measured reversal potentials plotted against log $[K^+]_o$. The dotted line is the best-fit linear regression to our data and the solid line is predicted under ideal K^+ conductance conditions, calculated with the Nernst equation at 20°C. (Results in *D* and *E* were corrected for a junction potential of 10.4 mV.)

3.5 K^+-channel mRNA expression of LA vs. LV fibroblasts

We compared the mRNA expression of Kv1.5 and Kv4.3 subunits, potential contributors to fibroblast Kv currents, in fibroblasts from both control and CHF dogs. The results are shown in *Figure 4*. LV fibroblasts expressed Kv1.5 and Kv4.3 subunits more strongly than LA fibroblasts in both control (Kv1.5: 1.23 ± 0.15 vs. 0.77 ± 0.10, $P < 0.001$; Kv4.3: 0.08 ± 0.011 vs. 0.05 ± 0.01, $P < 0.001$) and CHF dogs (Kv1.5: 0.73 ± 0.07 vs. 0.29 ± 0.04, $P < 0.001$; for Kv4.3: 0.057 ± 0.005 vs. 0.027 ± 0.003, $P < 0.001$). Of note, Kv1.5 mRNA expression was over 10-fold stronger than that of Kv4.3, consistent with the slowly inactivating properties of fibroblast Kv current. Consistent with Kv current down-regulation in CHF (*Figure 3*), CHF dogs expressed significantly less Kv1.5 in LA (smaller by 60%) and LV fibroblasts (smaller by 41%) compared with control. Kv4.3 mRNA expression was significantly smaller in CHF ($P < 0.05$) only for LV fibroblasts. The Kv1.5 subunit mRNA findings were compatible with the results of current recordings. We also measured the mRNA expression of KCa1.1 (BK_{Ca}), believed to underlie the functionally important Ca^{2+}-dependent K^+ current in fibroblasts.[12] KCa1.1 was more strongly expressed in LA vs. LV fibroblasts from both control (0.021 ± 0.003 vs. 0.007 ± 0.001, $P < 0.001$) and CHF dogs (0.021 ± 0.003 vs. 0.008 ± 0.002, $P < 0.01$). CHF did not change the mRNA expression of KCa1.1 compared with control. The mRNA expression of cardiac actin was also measured to exclude important contamination of fibroblast preparations by cardiomyocytes. As shown in Supplementary material online, *Figure S4*, cardiac actin was virtually undetectable in the fibroblast-enriched preparation.

3.6 K^+-channel blocker effects on fibroblast proliferation

To determine whether Kv current might contribute to the control of fibroblast function, we used ^{3}H-labelled thymidine incorporation as an index of fibroblast proliferation. Freshly isolated LA and LV fibroblasts were cultured for 4–5 days to acquire a large enough number of cells for the proliferation assay. The cells were then treated with medium containing different TEA concentrations (vehicle, 0.1 and 1 mmol/L) for 24 h. A statistically significant enhancement in fibroblast proliferation was noted at 1 mmol/L of TEA (*Figure 5A*), a concentration close to the IC_{50} for Kv-current inhibition. TEA-sensitive currents (at 1 mmol/L) were recorded in cultured fibroblasts at a time-point equivalent to that of TEA treatment (culture day 4–5). Substantial TEA-sensitive currents, which preserved significant LA–LV differences, were noted in cultured fibroblasts (*Figure 5B*). We also exposed cultured fibroblasts to 4-AP (300 μmol/L) or the highly selective Kv1.5 blocker S9947 (1 μmol/L). 4-AP exposure induced a significantly faster proliferation rate in LA fibroblasts (*Figure 5C*). S9947 also tended to increase LA fibroblast proliferation, but the results did not achieve statistical significance (*Figure 5C*). Like TEA-sensitive currents, 4-AP-sensitive currents in cultured fibroblasts preserved statistically significant LA–LV differences (*Figure 5D*).

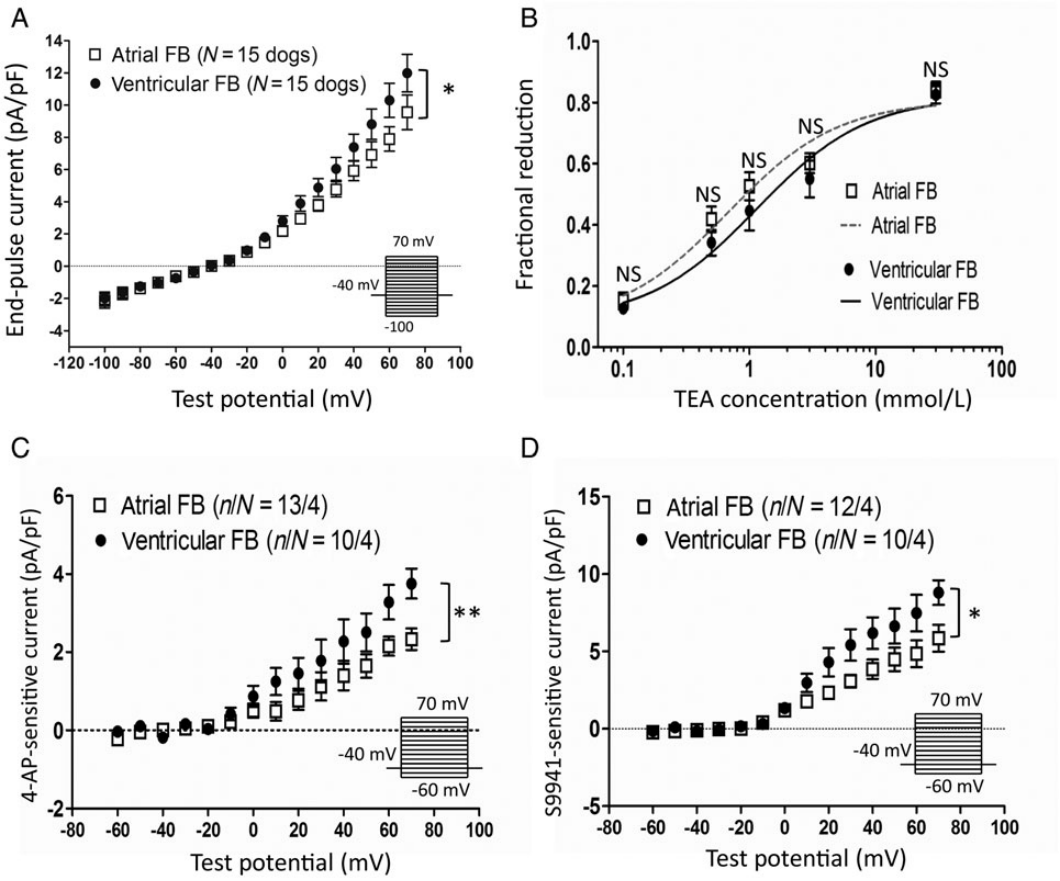

Figure 2 Baseline current densities and TEA response of control atrial and ventricular fibroblasts (FBs). (*A*) Current–density voltage relationships of atrial and ventricular FBs. The voltage-clamp protocol delivered at 0.1 Hz is shown in the inset. Dog-based current densities, obtained with the use of per-dog LA and LV values (results shown are from 50 atrial cells from 15 control dogs and 46 ventricular cells from the same dogs). (*B*) FBs were treated with different TEA concentrations, and the effect of TEA on total end-pulse current at +60 mV was expressed as a fractional reduction: $(I_{BL}-I_{TEA})/I_{BL}$, where I_{BL}, I_{TEA}, current under baseline, and TEA conditions, respectively. The calculated IC_{50} of TEA was 0.68 mmol/L for atrial and 1.15 mmol/L for ventricular FBs. (*C*) 4-AP- (300 μmol/L) and (*D*) S9947- (1 μmol/L) sensitive current densities for control LA and LV FBs. $^{*}P < 0.05$, $^{**}P < 0.01$ for atrial vs. ventricular FBs by two-way ANOVA. *n*/*N*, number of cells/number of dogs.

3.7 KCa1.1 current density and fibroblast proliferation

Since LA and LV fibroblasts manifested different expression levels of KCa1.1 (BK_{Ca}) mRNA, we used a selective BK_{Ca} channel blocker, paxilline,[18,19] to study this current. Calcium was included in the pipette solution (with calculated $[Ca^{2+}]_i = 100$ nmol/L) to activate BK_{Ca} channels. Paxilline was used at a concentration (1 μmol/L) much larger than the IC_{50} to ensure full block. The result (*Figure 6A*) shows significantly larger paxilline-sensitive currents in LA than in LV fibroblasts (e.g. 3.0 ± 0.5 LA vs. 1.6 ± 0.2 pA/pF LV at +60 mV, $P < 0.001$), compatible with the mRNA results in *Figure 4*. We also recorded paxilline-sensitive currents in cultured fibroblasts (Day 4–5), which showed no significant difference between LA and LV fibroblasts (*Figure 6B*). We then verified paxilline effects on proliferation by ^{3}H-thymidine assay (*Figure 6C*). LA fibroblasts treated with 0.1 μmol/L of paxilline showed greater proliferation comparing with vehicle. On the other hand, the effect of paxilline on LV fibroblasts was smaller and not statistically significant, compatible with the larger current densities in LA. At a higher concentration (1 μmol/L), the paxilline effect decreased and was no longer statistically significant.

4. Discussion

4.1 Summary of the major findings

In the present study, we assessed the expression of Kv currents in freshly isolated canine fibroblasts. Kv currents and corresponding subunit mRNA expression were strongly down-regulated in CHF fibroblasts, and mimicking Kv-current down-regulation with the Kv-current blocker enhanced fibroblast proliferation. We also noted differential Kv current and subunit mRNA expression in LA vs. LV fibroblasts, although the differences were much smaller than those observed for CHF vs. control. BK_{Ca} currents were smaller than TEA-sensitive Kv currents. They were also differentially expressed in LA vs. LV, but in contrast to Kv currents were more strongly expressed in LA.

4.2 Previous findings regarding ionic currents in cardiac fibroblasts

Li *et al.*[12] showed multiple ionic currents, including BK_{Ca}, transient-outward current (I_{to}), Kv current, inward-rectifier K^+ current (I_{Kir}), Cl^- current (I_{Cl}), L-type Ca^{2+} current (I_{CaL}), and Na^+

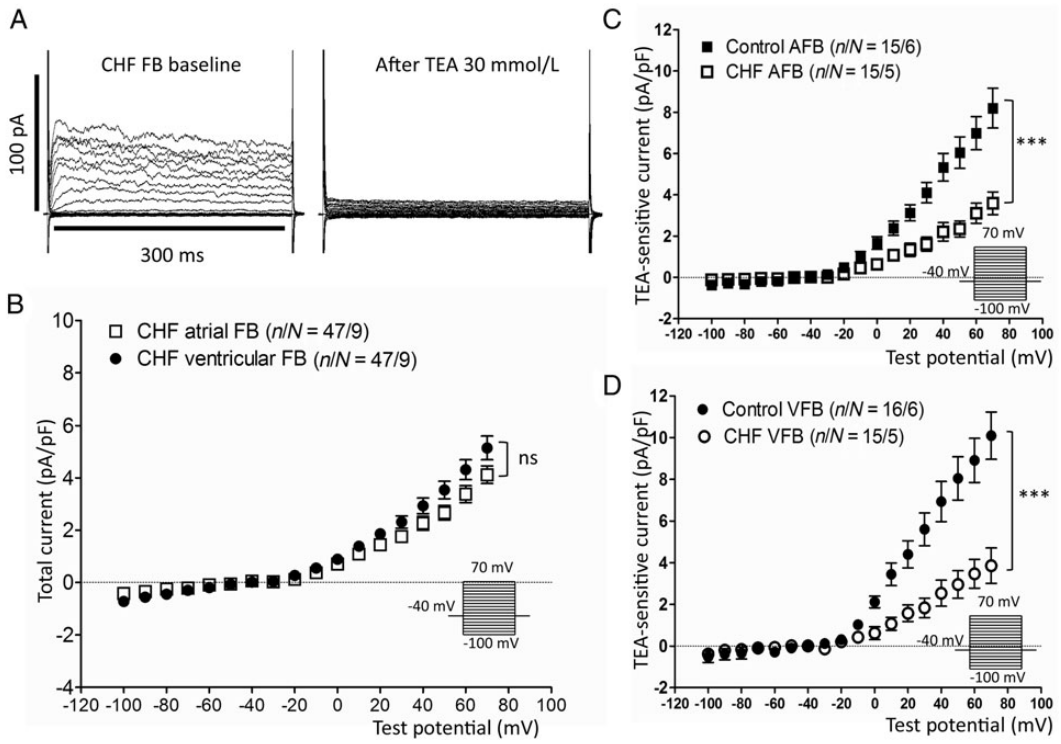

Figure 3 Kv-current properties of atrial and ventricular FBs from CHF dogs. (*A*) Representative current recordings from FBs from a CHF dog at baseline (left) and after treatment with 30 mmol/L of TEA (right). (*B*) Baseline current–density voltage relationships (expressed as total end-pulse current) for CHF atrial and ventricular FBs. The voltage-clamp protocol (inset) was delivered at 0.1 Hz. (*C*) and (*D*) Comparison of TEA-sensitive current densities (baseline current densities minus current densities in 30 mmol/L of TEA) between control and CHF dogs for both atrial (AFB) and ventricular FBs (VFB). ***$P < 0.001$ for control vs. CHF FBs by two-way ANOVA. *n*/*N*, number of cells/number of dogs.

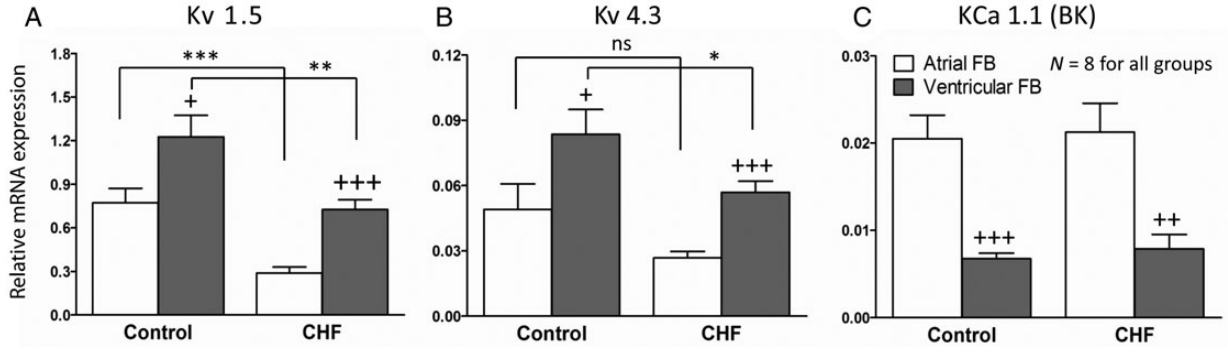

Figure 4 mRNA expression measured by qPCR for (*A*) Kv1.5, (*B*) Kv4.3, and (*C*) KCa1.1 subunits. Sample numbers were eight (dogs) for all groups. Comparison between control and CHF FBs: *$P < 0.05$, **$P < 0.01$, ***$P < 0.001$. Comparison between atrial and ventricular FBs: $^{+}P < 0.05$, $^{++}P < 0.01$, $^{+++}P < 0.001$. All comparisons were ANOVA with Bonferroni-corrected *t*-tests.

current (I_{Na}) in passage 2–6 cultured human ventricular fibroblasts. About 90% of cells expressed BK_{Ca} current, 15% expressed I_{to}, and 24% expressed I_{Kir}. The Kv currents they recorded were much smaller than BK_{Ca} current. This discrepancy from our findings may be due to the fact that they studied cultured fibroblasts, whereas here we assessed freshly isolated cells, and cell culture strongly down-regulates fibroblast Kv currents.[20] Chilton *et al.*[13] demonstrated both inward and outward K^+ currents in freshly isolated fibroblasts from adult rat ventricle. They focused primarily on inward I_{Kir}, which was Ba^{2+}-sensitive and controlled the resting potential. Of note, they did not detect down-regulation of Kv currents under culture conditions. The electrical properties of rat fibroblast outward K^+ currents were subsequently analysed in detail by the same group.[21] They noted current morphologies similar to those studied here: time-dependent activation and slow inactivation

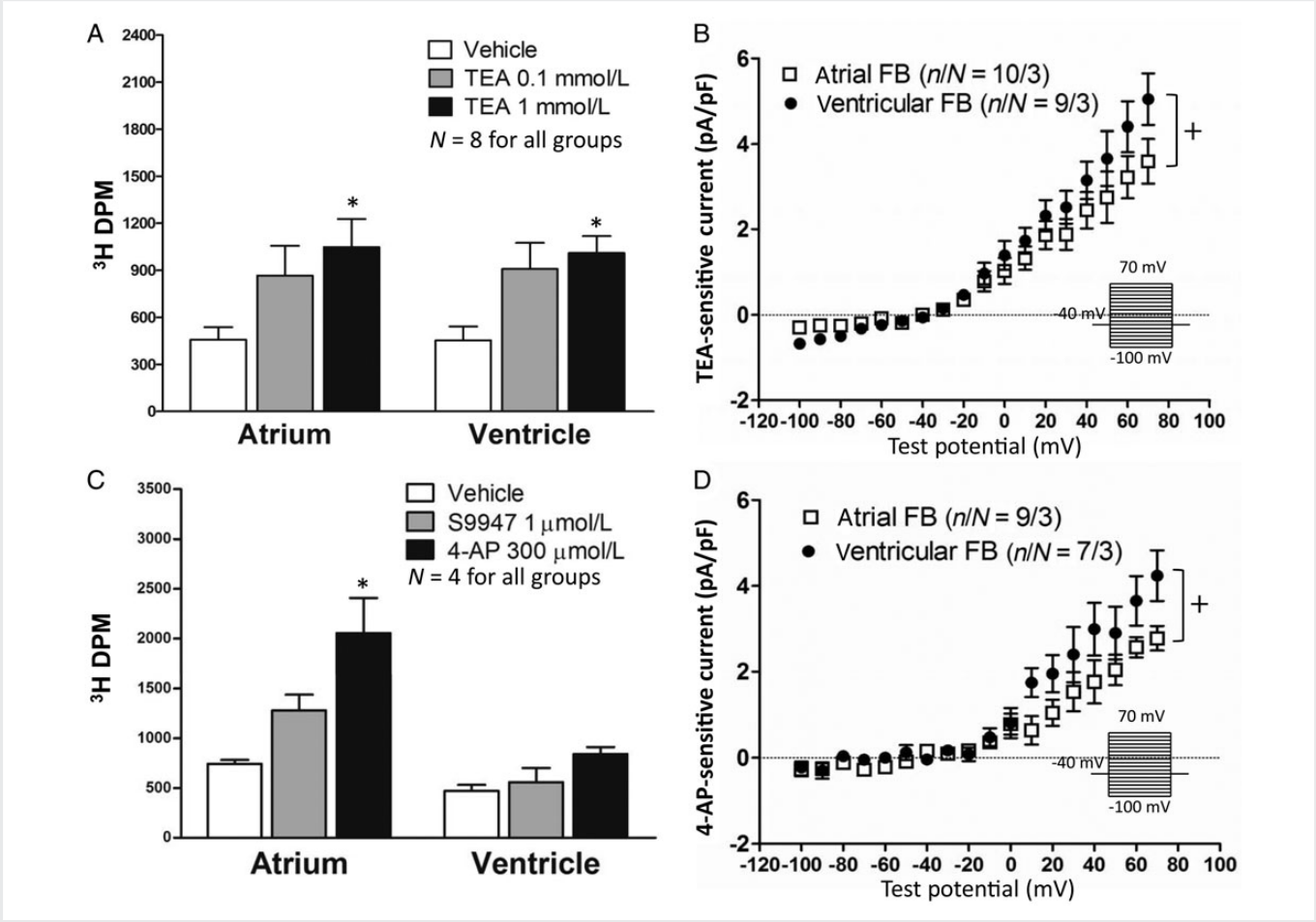

Figure 5 (Left) Effects of K^+-channel blockers on FB proliferation. (Right) Current–density voltage relationships in cultured FBs. (*A*) Results for TEA (0.1 and 1 mmol/L). (*B*) Results for 1 mmol/L of TEA-sensitive current density. (*C*) Results for 4-AP (300 μmol/L) and S9947 (1 μmol/L) effects on FB proliferation. (*D*) 4-AP-sensitive current densities (at 300 μmol/L). $^*P < 0.05$ by two-way ANOVA with Bonferroni *post hoc* test. $^+P < 0.05$ for LA vs. LV current densities, by two-way ANOVA. Left: *N*, number of dogs; Right: *n*/*N*, number of cells/number of dogs.

compatible with a C-type inactivation processes, strong K^+-selectivity and TEA-sensitivity.

4.3 Differential expression of ionic currents between atrial and ventricular fibroblasts

Chamber-specific gene expression patterns are well recognized in the heart.[22–24] However, cell specificity is less well appreciated. Previous work has indicated that atrial tissue is more vulnerable to fibrotic stimuli than ventricular.[14,15] About 25 years ago, Kardami and Fandrich[25] reported that the concentration of basic fibroblast growth factor is greater in atrial than ventricular tissue extracts. Burstein *et al.*[15] showed that cultured atrial fibroblasts show signs of myofibroblast differentiation more rapidly under culture conditions than ventricular fibroblasts. In the same study, microarrays revealed 225 differentially expressed genes between atrial and ventricular fibroblasts. Differences in PDGF receptor expression were shown to be of particular importance in the atrial–ventricular fibroblast behaviour differences. Here, we examined LA vs. LV fibroblast ion-channel expression and found that LA fibroblasts express less Kv current, but more BK_{Ca} current, than LV. Given the ability of Kv and BK_{Ca} current blockade to alter fibroblast proliferation, the differences we noted may influence atrial–ventricular differences in fibrosis. Theoretically, the smaller Kv current in LA vs. LV could promote fibrosis and contribute to the atrial pro-fibrotic tendency. However, the LA–LV Kv-current differences were small and only seen at quite positive potentials, so their functional importance is questionable. The BK_{Ca} differences would be expected to diminish the atrial fibrotic tendency based on the proliferation-enhancing effect we saw of 0.1 μmol/L of paxilline. Thus, BK_{Ca} may act as an internal check on atrial pro-fibrotic processes.

4.4 Potential significance of CHF-induced remodelling of fibroblast Kv channels

Although cardiac fibroblasts are non-excitable cells, they can act as important current sinks if coupled with cardiomyocytes.[26–28] Fibroblasts can act as mechano-electrical transducers, with stretch-activated channels on fibroblasts that can alter cardiomyocyte membrane potentials in pathological situations.[10,29] Fibroblasts have been shown to importantly affect cardiomyocyte electrical activity[8,30] and to induce arrhythmogenesis[31,32] in fibroblast–cardiomyocyte co-culture. Critical determinants of the effects of fibroblasts on cardiomyocyte electrical activity include the extent of coupling and the number of fibroblasts coupled with cardiomyocytes.[30–37] Disease-induced changes in

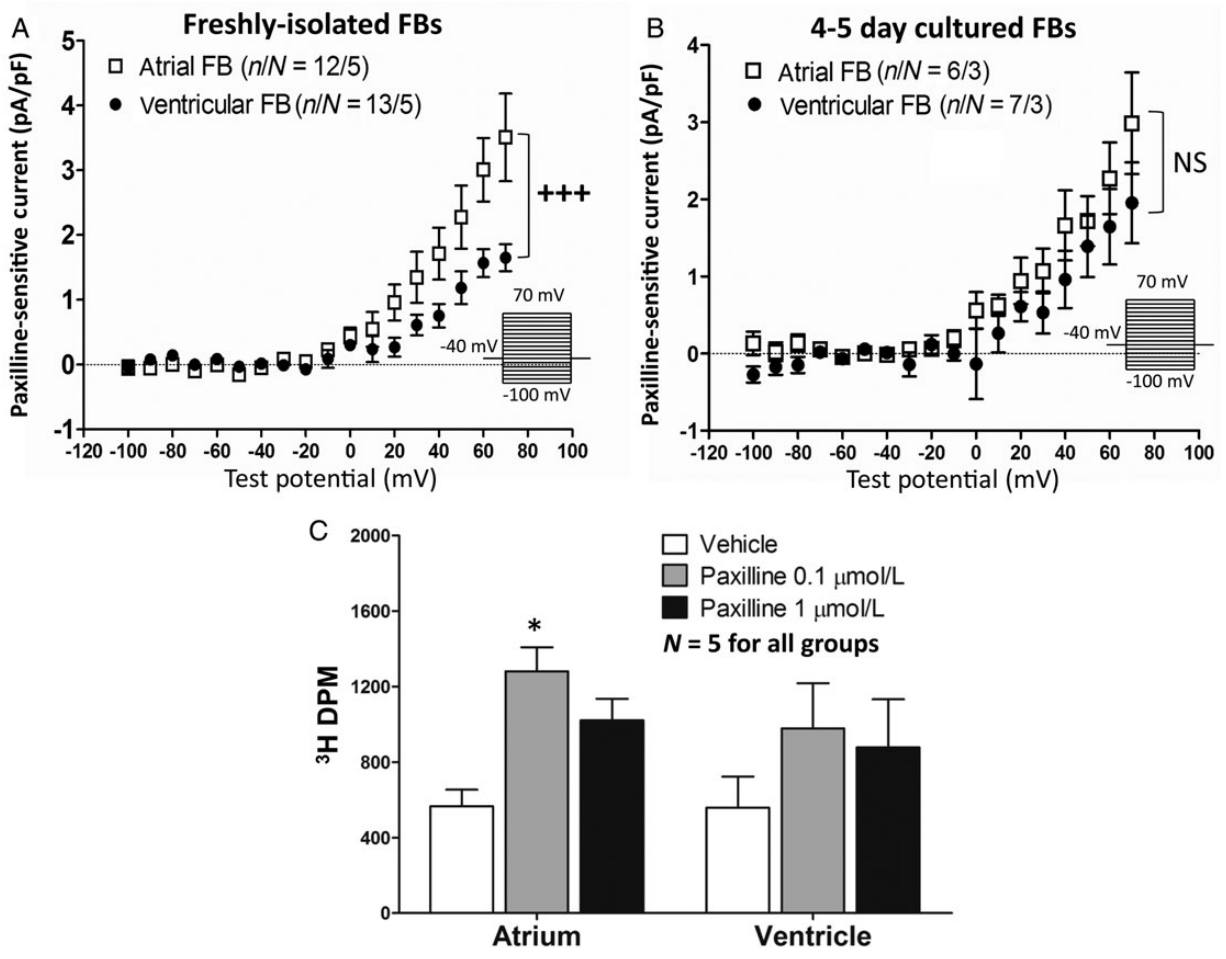

Figure 6 (*A*) Paxilline-sensitive current densities (control current densities minus current densities with 1-μmol/L of paxilline) for control atrial and ventricular FBs. Freshly isolated atrial and ventricular FBs (*A*) and after 4–5 day culture (*B*). Voltage-clamp protocol (0.1 Hz) is in inset. *n*/*N*, number of cells/number of dogs. (*C*) Paxilline effect on FB proliferation. Sample numbers were five (dogs) for all groups. $^{*}P < 0.05$ vs. baseline by two-way ANOVA with Bonferroni-corrected *t*-test. $^{+++}P < 0.001$ for atrial vs. ventricular FB current density, by two-way ANOVA.

fibroblast ion-channel function of the type we describe here have the capacity to influence the consequences of cardiomyocyte–fibroblast electrical interactions and associated arrhythmogenesis.

Another potentially important role of fibroblast ion channels is the regulation of fibroblast proliferation and associated fibrosis. There is evidence in the literature that changed fibroblast channel function can affect the pro-fibrotic properties of fibroblasts. In Alzheimer disease models, acute TEA exposure depolarizes fibroblast membrane potential, causes intracellular Ca^{2+} elevation, and enhances fibroblast proliferation.[38–40] In fibroblast-like synoviocytes, both paxilline (200 nmol/L) and TEA (5 mmol/L) increase intracellular calcium concentration.[41] In cultured human cardiac fibroblasts, both 1–3 μmol/L paxilline and KCa1.1 knockdown have been shown to suppress proliferation.[42] This finding differs from our observations with 0.1 μmol/L of paxilline.[42] Possible explanations of the discrepancy include species-specificity (human vs. dog) and differences in the preparation (5- to 6-day cultured cells in our study vs. second—sixth passage cultured human fibroblasts). To examine the role of Kv currents, we exposed cells to 0.1 and 1 mmol/L of TEA, the latter producing ~50% Kv-current inhibition (*Figure 2*), an effect of the order of that produced by CHF (*Figure 3*). We also used 4-AP and the selective Kv1.5 blocker S9947, obtaining qualitatively similar results, compatible with a contribution of Kv-current down-regulation to the well-recognized pro-fibrotic effects of CHF.

4.5 Novel elements of this study

To our knowledge, the present study is the first to examine atrial–ventricular differences in fibroblast ion-channel current and mRNA expression. It is also the first to explore the potential role of Kv currents in cardiac fibroblast function. Our results suggest that the reduced Kv-current expression resulting from CHF-induced remodelling of LA and LV fibroblasts may contribute to the fibrotic changes occurring at both the atrial and ventricular levels.

4.6 Study limitations

In the present study, we used freshly isolated cells rather than cultured cells in order to demonstrate the ionic currents under the most physiological conditions possible. While the proportion of myofibroblasts is small in freshly isolated cells, we cannot determine the extent to which myofibroblast transformation, particularly in CHF cells, might have contributed to our findings. The same general limitation also

applied to ^{3}H-thymidine assays. Because fibroblasts must be cultured for 4–5 days to obtain enough material for thymidine assay, fibroblast phenotype may have changed prior to assay.[20] It is possible that the isolation procedure affects fibroblast integrity. An underlying assumption is that any effects are similar on control and CHF fibroblasts.

Pharmacological approaches were used to characterize the currents observed. TEA and 4-AP were employed as classical K^+-channel blockers that have been used extensively to study voltage-gated K^+ channels. S9947 and paxilline were used as established selective blockers for currents carried by Kv1.5[17] and BK_{Ca}[18,19] subunits, respectively. S9947 inhibits Kv1.5 currents in CHO cells with an IC_{50} of 0.42 μmol/L. Inhibition of Kv4.3 and HERG currents is ∼20% at 10 μmol/L S9947.[17] Paxilline has an IC_{50} for BK_{Ca} current of ∼2 nmol/L.[35] At higher concentrations, of the order of 5–50 μmol/L, paxilline can also block sarco-/endoplasmic reticulum Ca^{2+}–ATPase and affect intracellular signalling.[19] Such non-specific effects may explain why the effect of paxilline on fibroblast proliferation decreased, becoming statistically non-significant, at 1 μmol/L in our study. We used NaCl to replace KCl to maintain osmotic balance when varying $[K^+]_e$—we cannot exclude an effect on ion balances by permeation through non-selective cation channels, although cell dialysis with pipette solution should minimize ion-concentration changes.

Although LA fibroblast currents were smaller than LV, the proliferation-enhancing effect of Kv-current blockade was greater in LA cells. This observation may reflect the generally greater response of LA vs. LV fibroblasts to a wide range of pro-fibrotic stimuli.[15]

We worked with random-source mongrel dogs, and had no reliable information about their age. Fibrosis increases with aging, and fibroblast properties may also change with aging. Since animal age was unknown, it is possible that age differences between groups could have affected results.

We quantified ion-channel subunit changes by qPCR measurements of mRNA expression only. We attempted to quantify protein expression with western blots, but were unable to obtain results of sufficient quality with commercially available antibodies and the relatively small amount of protein we could obtain from freshly isolated fibroblasts. This lack of protein expression data should be considered in interpreting our findings.

Supplementary material

Supplementary material is available at *Cardiovascular Research* online.

Acknowledgements

The authors thank Chantal St-Cyr and Nathalie L'Heureux for technical help, and France Thériault for secretarial help with the manuscript.

Conflict of interest: none declared.

Funding

This work was supported by the Canadian Institutes of Health Research (MOP44365, 68929) and the Canadian Heart and Stroke Foundation.

References

1. Nag A. Study of non-muscle cells of the adult mammalian heart: a fine structural analysis and distribution. *Cytobios* 1980;**28**:41–61.
2. Pedrotty DM, Klinger RY, Kirkton RD, Bursac N. Cardiac fibroblast paracrine factors alter impulse conduction and ion channel expression of neonatal rat cardiomyocytes. *Cardiovasc Res* 2009;**83**:688–697.
3. Camelliti P, Borg TK, Kohl P. Structural and functional characterisation of cardiac fibroblasts. *Cardiovasc Res* 2005;**65**:40–51.
4. Yue L, Xie J, Nattel S. Molecular determinants of cardiac fibroblast electrical function and therapeutic implications for atrial fibrillation. *Cardiovasc Res* 2011;**89**:744–753.
5. Burstein B, Comtois P, Michael G, Nishida K, Villeneuve L, Yeh YH, Nattel S. Changes in connexin expression and the atrial fibrillation substrate in congestive heart failure. *Circ Res* 2009;**105**:1213–1222.
6. Kawara T, Derksen R, de Groot JR, Coronel R, Tasseron S, Linnenbank AC, Hauer RN, Kirkels H, Janse MJ, de Bakker JM. Activation delay after premature stimulation in chronically diseased human myocardium relates to the architecture of interstitial fibrosis. *Circulation* 2001;**104**:3069–3075.
7. Camelliti P, Green CR, LeGrice I, Kohl P. Fibroblast network in rabbit sinoatrial node: structural and functional identification of homogeneous and heterogeneous cell coupling. *Circ Res* 2004;**94**:828–835.
8. Gaudesius G, Miragoli M, Thomas SP, Rohr S. Coupling of cardiac electrical activity over extended distances by fibroblasts of cardiac origin. *Circ Res* 2003;**93**:421–428.
9. Kohl P, Camelliti P. Fibroblast-myocyte connections in the heart. *Heart Rhythm* 2012;**9**:461–464.
10. Kamkin A, Kiseleva I, Isenberg G, Wagner KD, Günther J, Theres H, Scholz H. Cardiac fibroblasts and the mechano-electric feedback mechanism in healthy and diseased hearts. *Prog Biophys Mol Biol* 2003;**82**:111–120.
11. Kamkin A, Kiseleva I, Lozinsky I, Scholz H. Electrical interaction of mechanosensitive fibroblasts and myocytes in the heart. *Basic Res Cardiol* 2005;**100**:337–345.
12. Li GR, Sun HY, Chen JB, Zhou Y, Tse HF, Lau CP. Characterization of multiple ion channels in cultured human cardiac fibroblasts. *PLoS ONE* 2009;**4**:1–10.
13. Chilton L, Ohya S, Freed D, George E, Drobic V, Giles WR. K^+ currents regulate the resting membrane potential, proliferation, and contractile responses in ventricular fibroblasts and myofibroblasts. *Am J Physiol Heart Circ Physiol* 2005;**288**:H2931–H2939.
14. Hanna N, Cardin S, Leung TK, Nattel S. Differences in atrial versus ventricular remodeling in dogs with ventricular tachypacing-induced congestive heart failure. *Cardiovasc Res* 2004;**63**:236–244.
15. Burstein B, Libby E, Calderone A, Nattel S. Differential behaviors of atrial versus ventricular fibroblasts: a potential role for platelet-derived growth factor in atrial-ventricular remodeling differences. *Circulation* 2008;**117**:1630–1641.
16. Li D, Fareh S, Leung TK, Nattel S. Promotion of atrial fibrillation by heart failure in dogs: atrial remodeling of a different sort. *Circulation* 1999;**100**:87–95.
17. Bachmann A, Gutcher I, Kopp K, Brendel J, Bosch RF, Busch AE, Gögelein H. Characterization of a novel Kv1.5 channel blocker in Xenopus oocytes, CHO cells, human and rat cardiomyocytes. *Naunyn Schmiedebergs Arch Pharmacol* 2001;**364**:472–478.
18. Li G, Cheung DW. Effects of paxilline on K^+ channels in rat mesenteric arterial cells. *Eur J Pharmacol* 1999;**372**:103–107.
19. Sanchez M, McManus OB. Paxilline inhibition of the alpha-subunit of the high-conductance calcium-activated potassium channel. *Neuropharmacology* 1996;**35**:963–968.
20. Dawson K, Wu CT, Qi XY, Nattel S. Congestive heart failure effects on atrial fibroblast phenotype: differences between freshly-isolated and cultured cells. *PLoS ONE* 2012;**7**:e52032.
21. Shibukawa Y, Chilton EL, MacCannell KA, Clark RB, Giles WR. K^+ currents activated by depolarization in cardiac fibroblasts. *Biophys J* 2005;**88**:3924–3935.
22. Tabibiazar R, Wagner RA, Liao A, Quertermous T. Transcriptional profiling of the heart reveals chamber-specific gene expression patterns. *Circ Res* 2003;**93**:1193–1201.
23. Ellinghaus P, Scheubel RJ, Dobrev D, Ravens U, Holtz J, Huetter J, Nielsch U, Morawietz H. Comparing the global mRNA expression profile of human atrial and ventricular myocardium with high-density oligonucleotide arrays. *J Thorac Cardiovasc Surg* 2005;**129**:1383–1390.
24. Gaborit N, Le Bouter S, Szuts V, Varro A, Escande D, Nattel S, Demolombe S. Regional and tissue specific transcript signatures of ion channel genes in the non-diseased human heart. *J Physiol* 2007;**582**:675–693.
25. Kardami E, Fandrich RR. Basic fibroblast growth factor in atria and ventricles of the vertebrate heart. *J Cell Biol* 1989;**109**:1865–1875.
26. Goldsmith EC, Hoffman A, Morales MO, Potts JD, Price RL, McFadden A, Rice M, Borg TK. Organization of fibroblasts in the heart. *Dev Dyn* 2004;**230**:787–794.
27. Rook MB, van Ginneken AC, de Jonge B, el Aoumari A, Gros D, Jongsma HJ. Differences in gap junction channels between cardiac myocytes, fibroblasts, and heterologous pairs. *Am J Physiol* 1992;**263**:C959–C977.
28. Vasquez C, Mohandas P, Louie KL, Benamer N, Bapat AC, Morley GE. Enhanced fibroblast-myocyte interactions in response to cardiac injury. *Circ Res* 2010;**107**:1011–1020.
29. Xie Y, Garfinkel A, Camelliti P, Kohl P, Weiss JN, Qu Z. Effects of fibroblast-myocyte coupling on cardiac conduction and vulnerability to reentry: a computational study. *Heart Rhythm* 2009;**6**:1641–1649.
30. Thompson SA, Copeland CR, Reich DH, Tung L. Mechanical coupling between myofibroblasts and cardiomyocytes slows electric conduction in fibrotic cell monolayers. *Circulation* 2011;**123**:2083–2093.
31. Miragoli M, Salvarani N, Rohr S. Myofibroblasts induce ectopic activity in cardiac tissue. *Circ Res* 2007;**101**:755–758.
32. Zlochiver S, Munoz V, Vikstrom KL, Taffet SM, Berenfeld O, Jalife J. Electrotonic myofibroblast-to-myocyte coupling increases propensity to reentrant arrhythmias in two-dimensional cardiac monolayers. *Biophys J* 2008;**95**:4469–4480.

33. Jacquemet V, Henriquez CS. Loading effect of fibroblast-myocyte coupling on resting potential, impulse propagation, and repolarization: insights from a microstructure model. *Am J Physiol Heart Circ Physiol* 2008;**294**:H2040–H2052.
34. Sachse FB, Moreno AP, Seemann G, Abildskov JA. A model of electrical conduction in cardiac tissue including fibroblasts. *Ann Biomed Eng* 2009;**37**:874–889.
35. Xie Y, Garfinkel A, Weiss JN, Qu Z. Cardiac alternans induced by fibroblast-myocyte coupling: mechanistic insights from computational models. *Am J Physiol Heart Circ Physiol* 2009;**297**:H775–H784.
36. Maleckar MM, Greenstein JL, Giles WR, Trayanova NA. Electrotonic coupling between human atrial myocytes and fibroblasts alters myocyte excitability and repolarization. *Biophys J* 2009;**97**:2179–2190.
37. Ashihara T, Haraguchi R, Nakazawa K, Namba T, Ikeda T, Nakazawa Y, Ozawa T, Ito M, Horie M, Trayanova NA. The role of fibroblasts in complex fractionated electrograms during persistent/permanent atrial fibrillation: implications for electrogram-based catheter ablation. *Circ Res* 2012;**110**:275–284.
38. Tomasek JJ, Abbiani G, Hinz B, Chaponnier C, Brown RA. Myofibroblasts and mechano-regulation of connective tissue remodeling. *Nat Rev Mol Cell Biol* 2002;**3**:349–363.
39. Failli P, Tesco G, Ruocco C, Ginestroni A, Amaducci L, Giotti A, Sorbi S. The effect of tetraethylammonium on intracellular calcium concentration in Alzheimer's disease fibroblasts with APP, S182 and E5-1 missense mutations. *Neurosci Lett* 1996;**208**:216–218.
40. Etcheberrigaray R, Ito E, Oka K, Tofel-Grehl B, Gibson GE, Alkon DL. Potassium channel dysfunction in fibroblasts identifies patients with Alzheimer disease. *Proc Natl Acad Sci USA* 1993;**90**:8209–8213.
41. Hu X, Laragione T, Sun L, Koshy S, Jones KR, Ismailov II, Yotnda P, Horrigan FT, Gulko PS, Beeton C. KCa1.1 potassium channels regulate key proinflammatory and invasive properties of fibroblast-like synoviocytes in rheumatoid arthritis. *J Biol Chem* 2012;**287**:4014–4022.
42. He ML, Liu WJ, Sun HY, Wu W, Liu J, Tse HF, Lau CP, Li GR. Effects of ion channels on proliferation in cultured human cardiac fibroblasts. *J Mol Cell Cardiol* 2011;**51**:198–206.